

Merger of Neutron Stars: From Gravitational Waves to the Equation of State

SuperMUC Status and Results Workshop at the LRZ in Garching

April 26-27, 2016

*Luciano Rezzolla, Horst Stöcker, Marcio de Avellar, Matthias Hanauske,
Antonios Nathanail, Yosuke Mizuno, Oliver Porth, Ziri Younsi, Kentaro
Takami, Bruno Mundim, Elias Most, Sven Köppel, Ludwig Jens Papenfort,
Hector Olivares, Cosima Breu, Luke Bovard
and Federico Guercilena*

*Frankfurt Institute for Advanced Studies
Johann Wolfgang Goethe-University
Institute for Theoretical Physics
Department of Relativistic Astrophysics
Frankfurt am Main, Germany*

Merger of Neutron Stars: From Gravitational Waves to the Equation of State

1. Introduction
2. The Einstein Equation
3. The Equation of State of Neutron Star Matter
4. Numerical Relativity of Neutron Star Mergers
5. From Gravitational Waves to the Equation of State
6. Summary

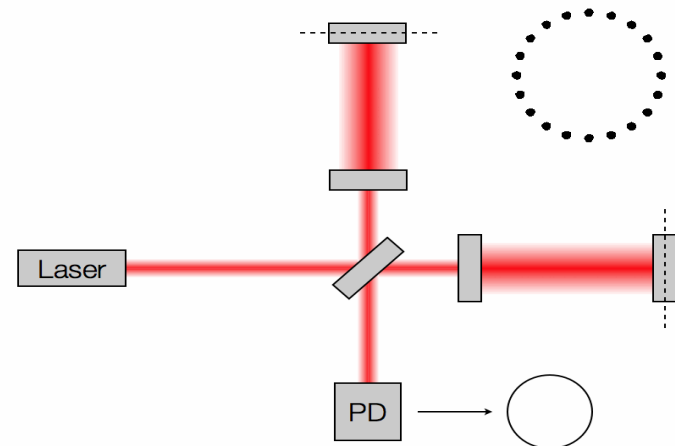
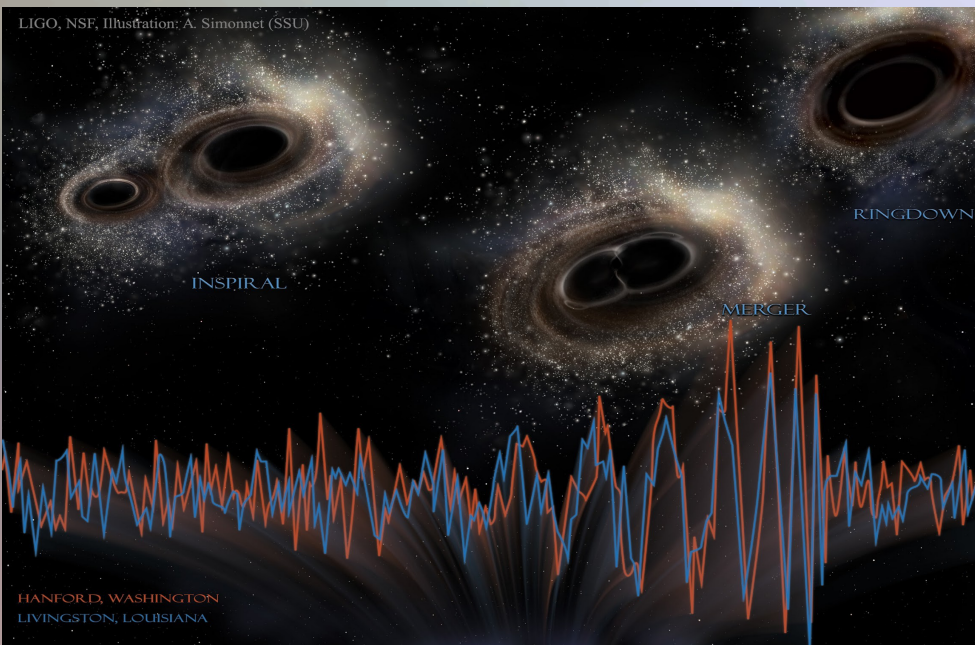
First observation gravitational waves from binary black hole merger by LIGO

Facts about GW150914

Merger of two black holes of around
36 and 29 solar masses

Energy released during the merger:
3 solar masses

Distance: 410 Mpc (1340 million Ly)



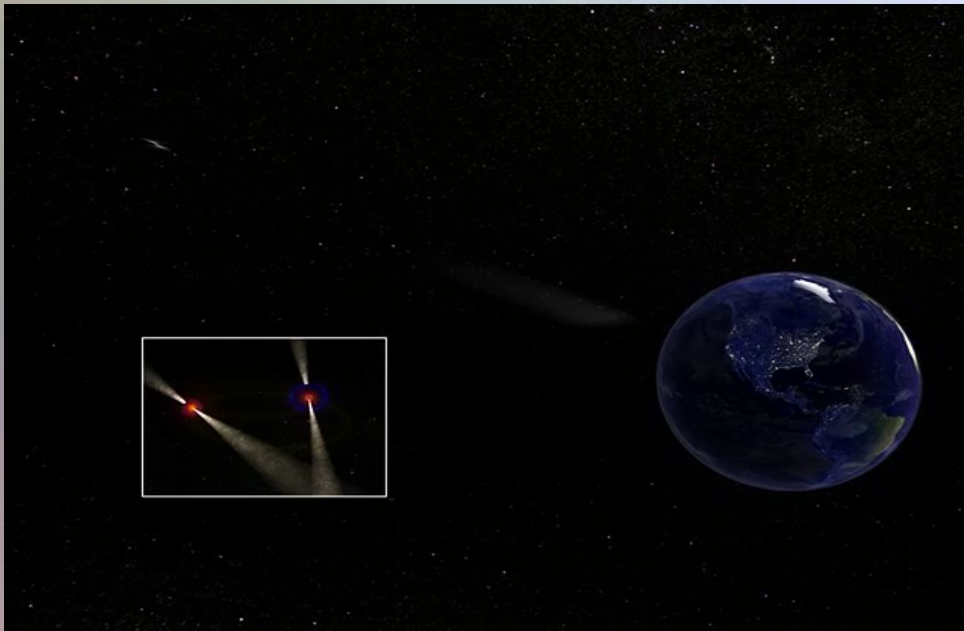
Credit: Les Wade from Kenyon College.

Neutron Stars (NS) ↔ Pulsars

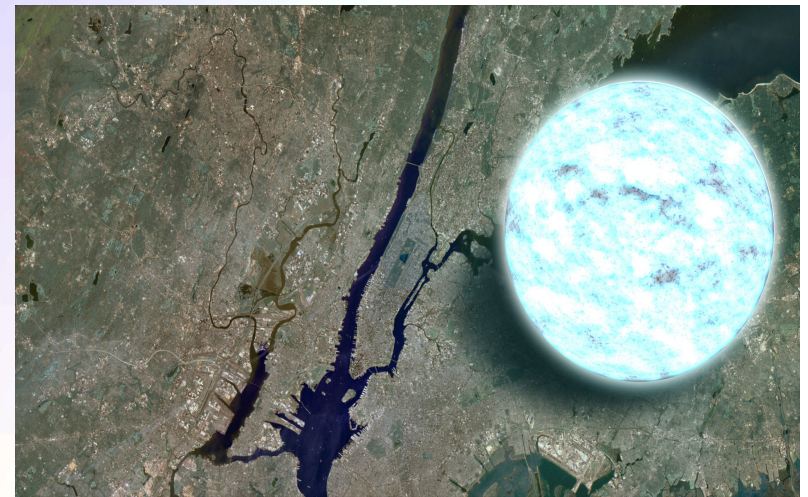
~ 2500 neutron stars are known, large magnetic fields (up to 10^{11} Tesla), fast rotation (up to 700 rotations/second), radius ~10 km, mass 1-2 solar masses.

Some NS are in binary systems (NS-planet, NS-(white dwarf) or NS-NS).

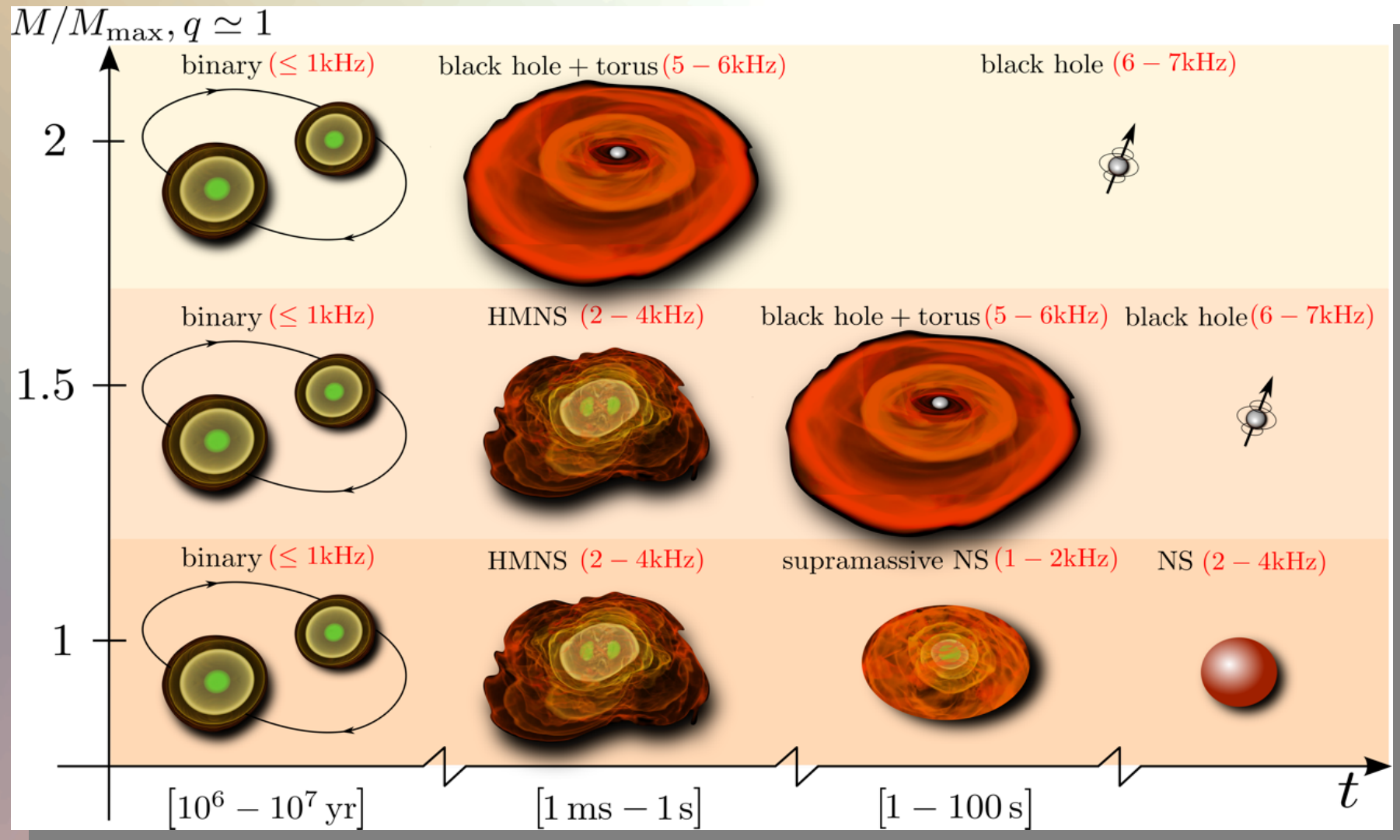
Double Pulsar (PSR J0737-3039A/B), discovered in 2003, separated only by 800,000 km, orbital period of 147 minutes, Periodic eclipse of one pulsar by the other, emission of gravitational waves → will merge in 85 million years.



Size of a neutron star compared to
New York



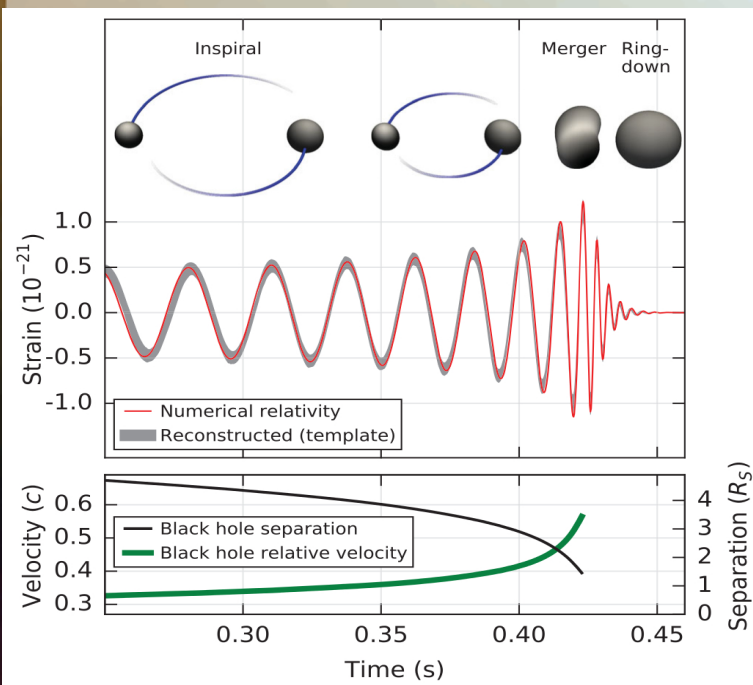
The Neutron Star Merger Product



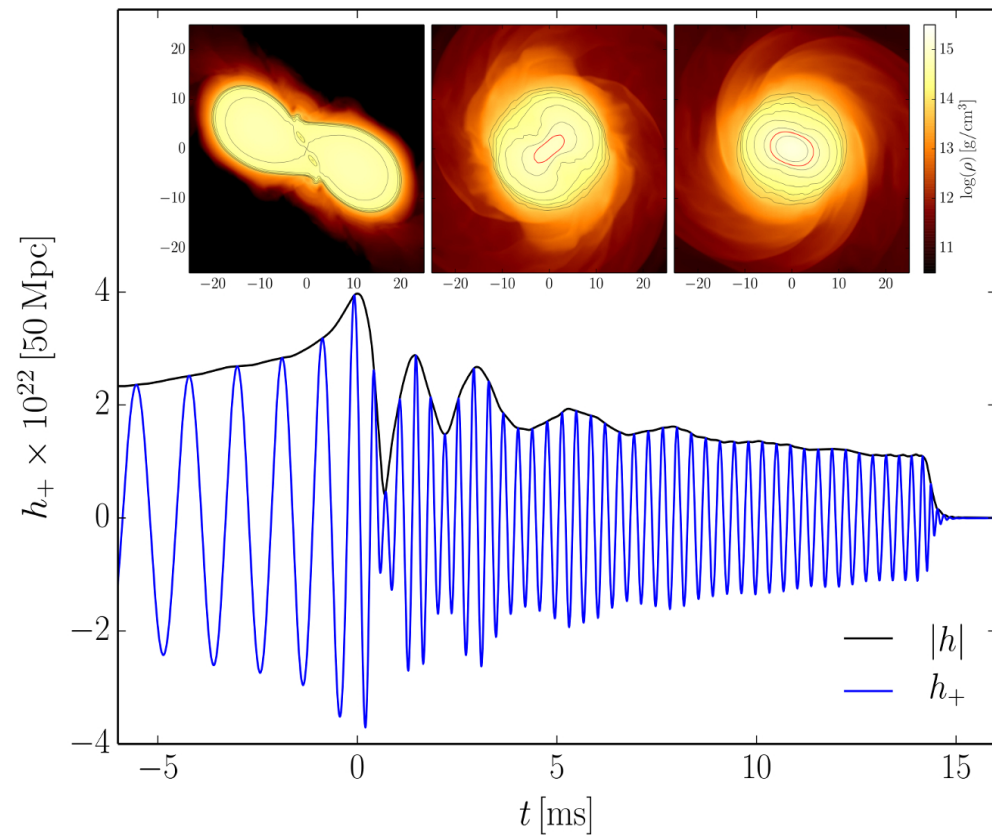
GWs from Neutron Star Mergers

Simulation of Gravitational Waves from Neutron Star Merger

Observed binary black hole merger by LIGO



Estimated gravitational-wave strain amplitude from GW150914.



Simulated gravitational wave amplitude h_+ and $|h|$ at a distance of 50 Mpc.

The Einstein Equation

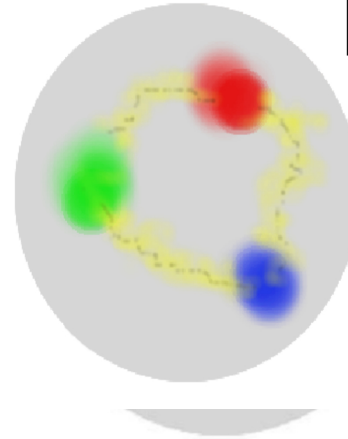
ART	Yang-Mills-Theories
$D_\beta v^\alpha = \partial_\beta v^\alpha + \Gamma_{\sigma\beta}^\alpha v^\sigma$	$D_{\beta a}{}^b = \partial_\beta 1_a{}^b + ig A_{\beta a}{}^b$
$R^\delta{}_{\mu\alpha\beta} v^\mu = [D_\alpha, D_\beta] v^\delta$	$F_{\alpha\beta a}{}^b = \frac{1}{ig} [D_{\alpha a}{}^c, D_{\beta c}{}^b]$
$R^\delta{}_{\mu\alpha\beta} = \Gamma_{\mu\alpha \beta}^\delta - \Gamma_{\mu\beta \alpha}^\delta$ $+ \Gamma_{\nu\beta}^\delta \Gamma_{\mu\alpha}^\nu + \Gamma_{\nu\alpha}^\delta \Gamma_{\mu\beta}^\nu$	$= A_{\beta a}{}^b{}_{ \alpha} - A_{\alpha a}{}^b{}_{ \beta}$ $+ \frac{1}{ig} [A_{\alpha a}{}^c, A_{\beta c}{}^b]$
$\mathcal{L}_G = R + \underbrace{(c_1 R_{\mu\nu} R^{\mu\nu} + \dots)}_{\equiv 0 \text{ for ART}}$	$\mathcal{L}_{YM} = \frac{1}{4} F_{\mu\nu a}{}^b F^{\mu\nu}{}_a{}^b$

Quantum Chromodynamic:

($SU(3)_{(c)}$ - Color Yang-Mills-Gauge Theory)

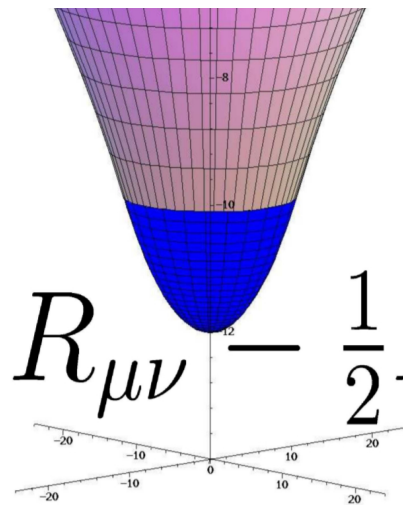
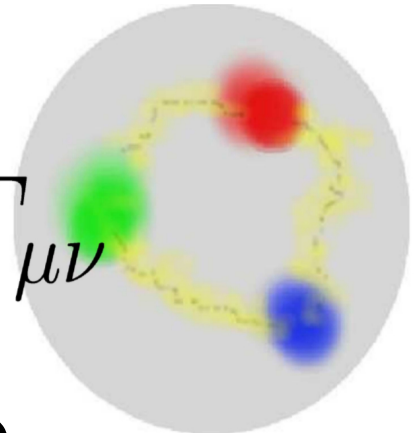
$$D_{\beta A}{}^B = \partial_\beta 1_A{}^B + ig G_{\beta A}{}^B$$

$A, B = \text{red, green, blue}$



$$\psi_A^f = \begin{pmatrix} \psi_r^f \\ \psi_g^f \\ \psi_b^f \end{pmatrix}$$

Confinement
chiral symmetry, ...

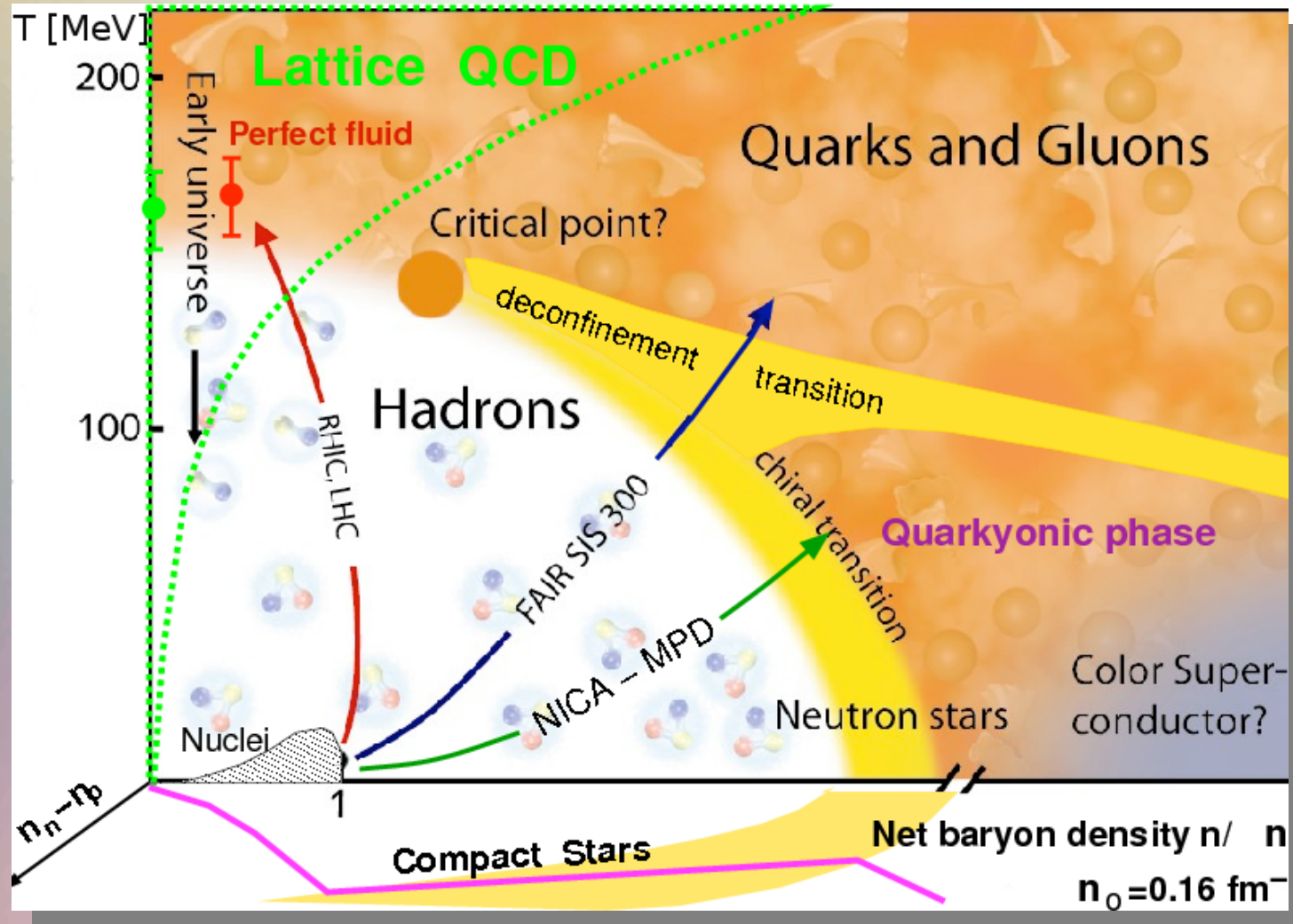


$$R_{\mu\nu} - \frac{1}{2} R g_{\mu\nu} =$$

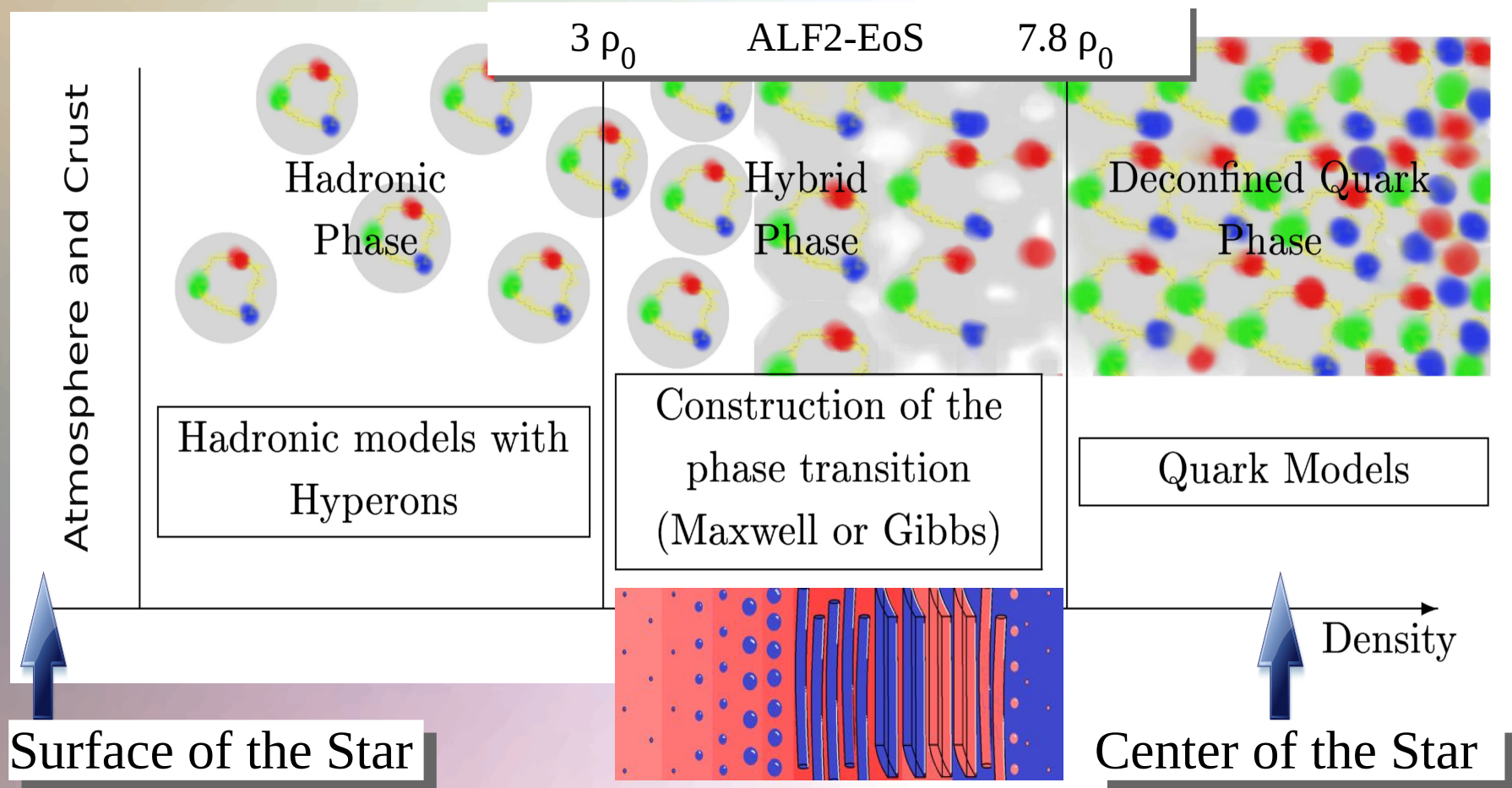
$$\frac{8\pi G}{c^4} T_{\mu\nu}$$

EOS: $P(\rho, T)$

The Equation of State and the QCD Phase Diagram



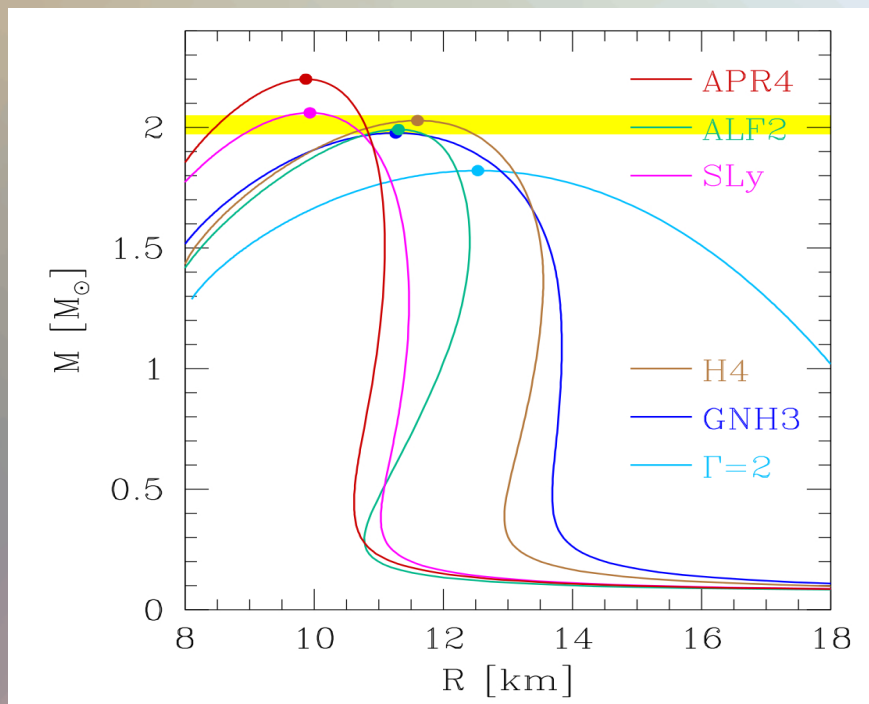
The QCD – Phase Transition and the Interior of a Hybrid Star



See: *Stable hybrid stars within a SU(3) Quark-Meson-Model*,
A.Zacchi, M.Hanuske, J.Schaffner-Bielich, PRD 93, 065011 (2016)

Numerical Setup

Several different EOSs : ALF2, APR4, GNH3, H4 and Sly, approximated by piecewise polytopes.



Thermal ideal fluid component ($\Gamma=2$) added to the nuclear-physics EOSs.

BSSNOK conformal traceless formulation of the ADM equations. 3+1 Valencia formulation and high resolution shock capturing methods for the hydrodynamic evolution. Full general relativity using the **Einstein-Toolkit** and the **WHISKY code** for the general-relativistic hydrodynamic equations.

Grid Structure:

Adaptive mesh refinement (six ref. levels)

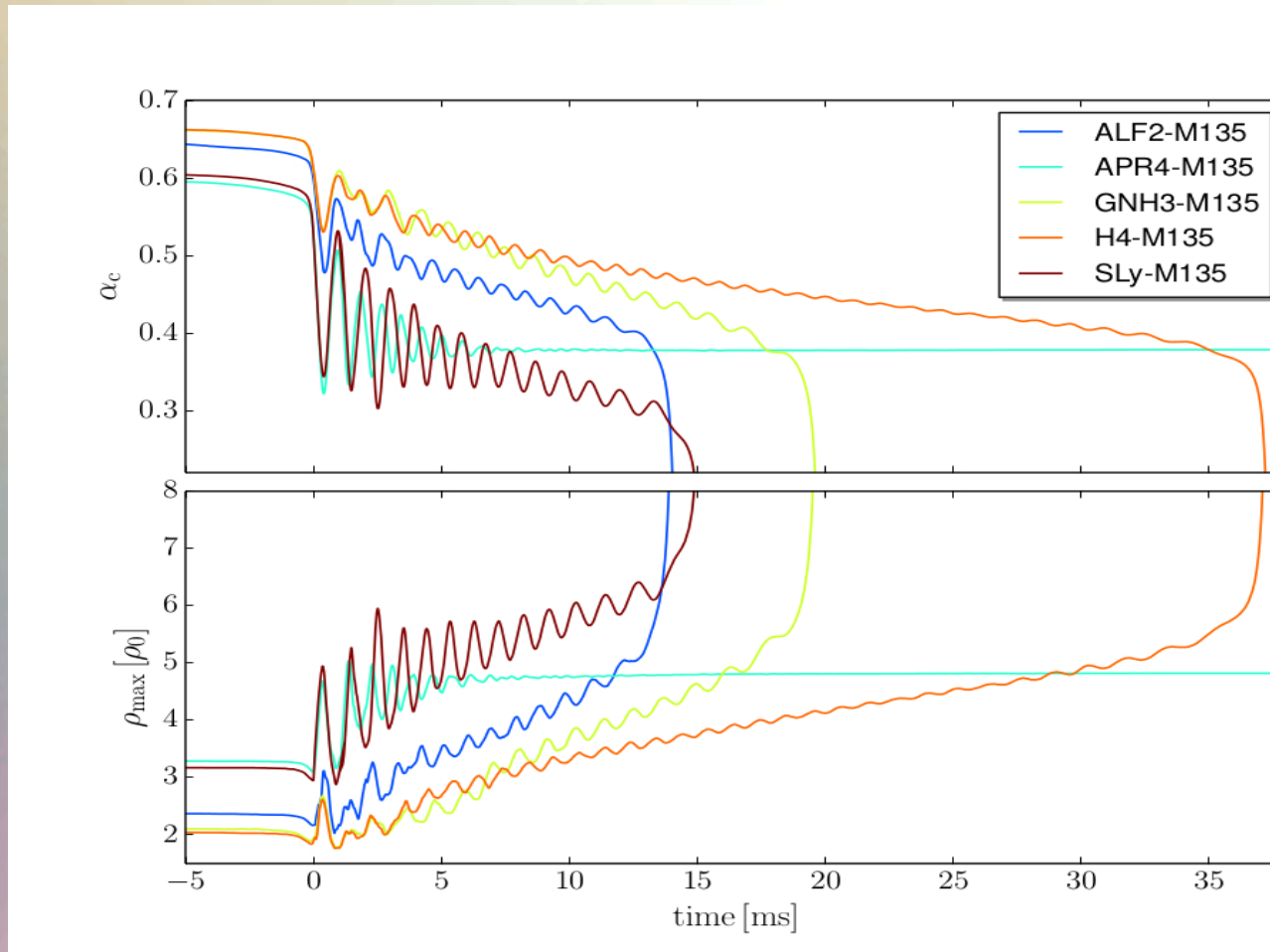
Grid resolution: (from 221 m to 7.1 km)

Outer Boundary: 759 km

Initial separation of stellar cores: 45 km

HMNS Evolution for different EoSs

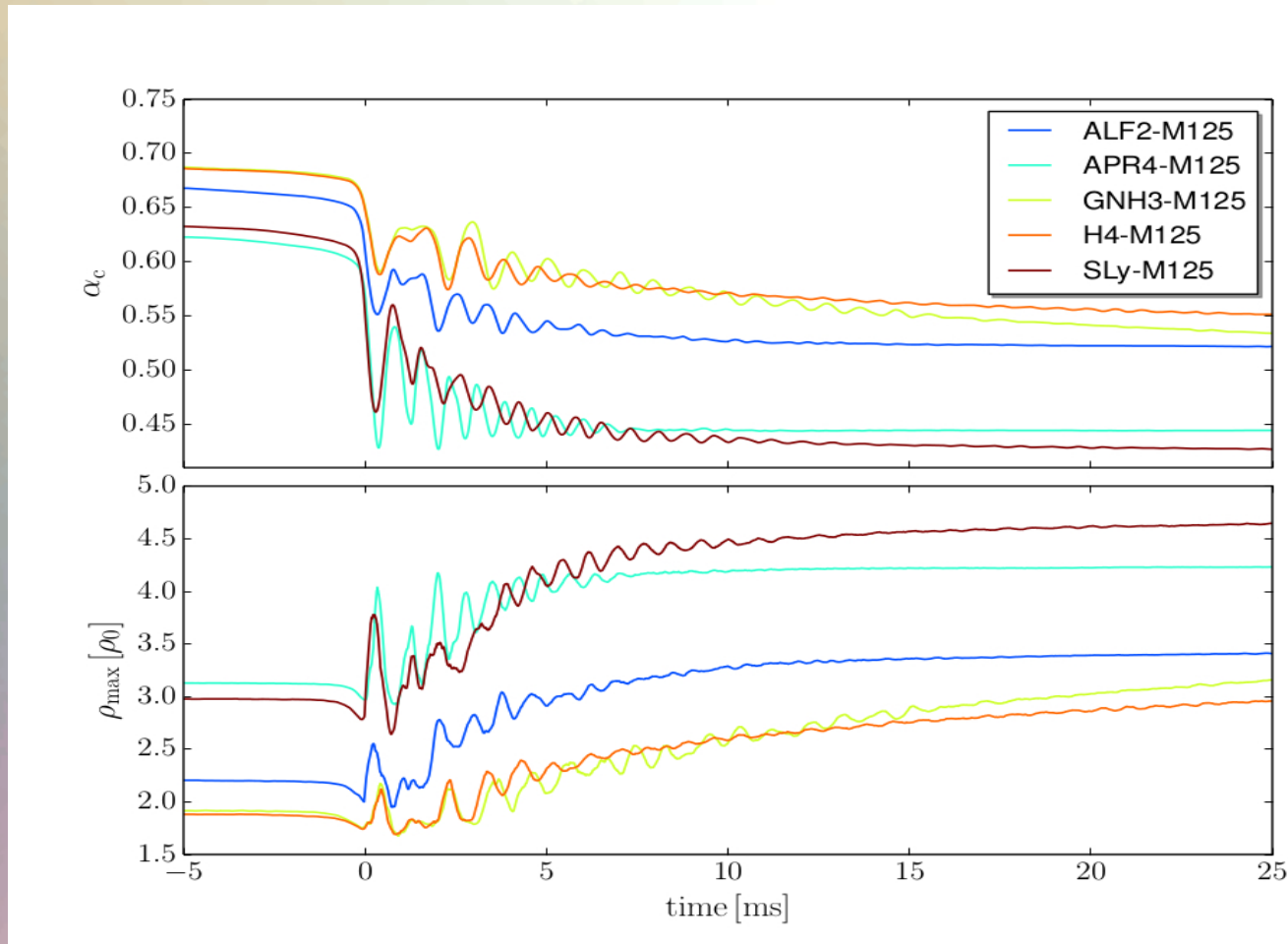
High mass simulations (M=1.35)



Central value of the lapse function α_c (upper panel) and maximum of the rest mass density ρ_{\max} in units of ρ_0 (lower panel) versus time for the high mass simulations.

HMNS Evolution for different EoSs

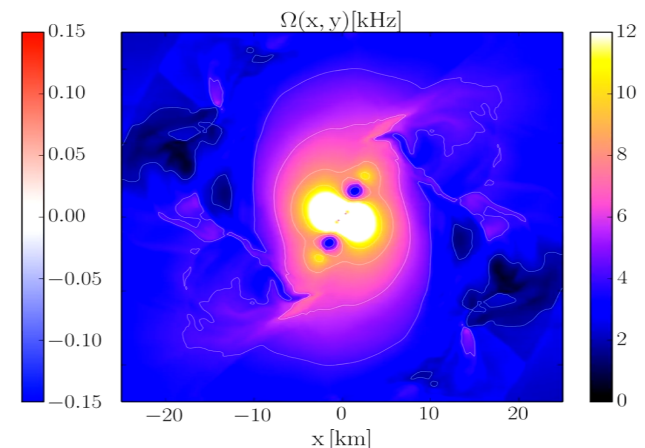
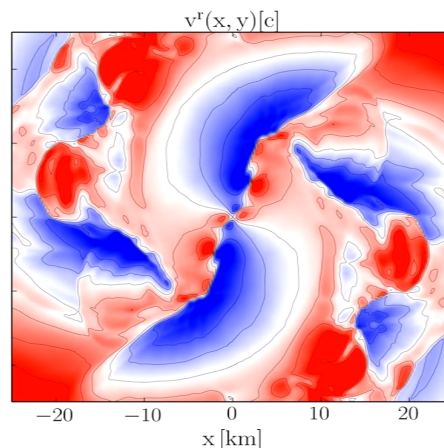
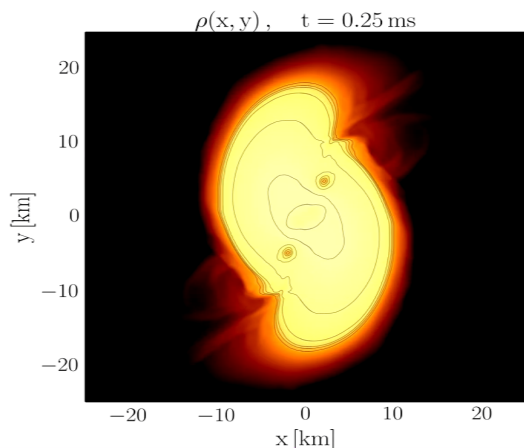
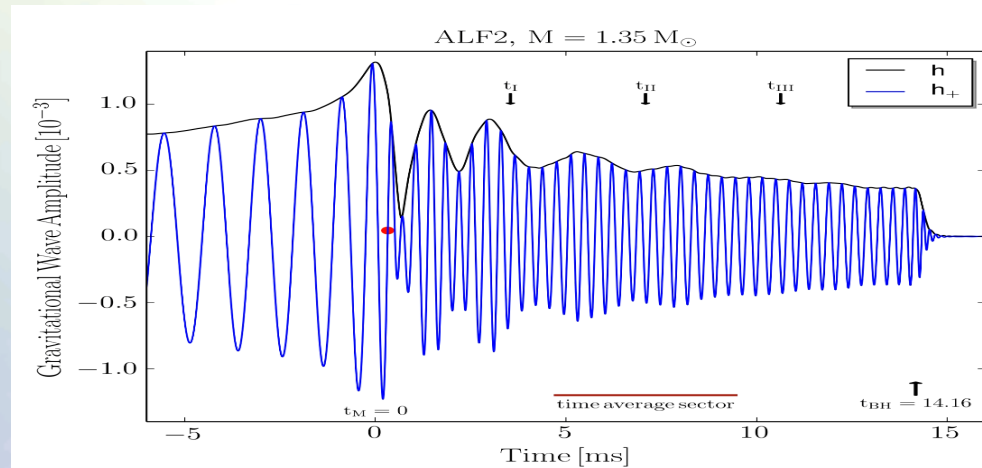
Low mass simulations ($M=1.25$)



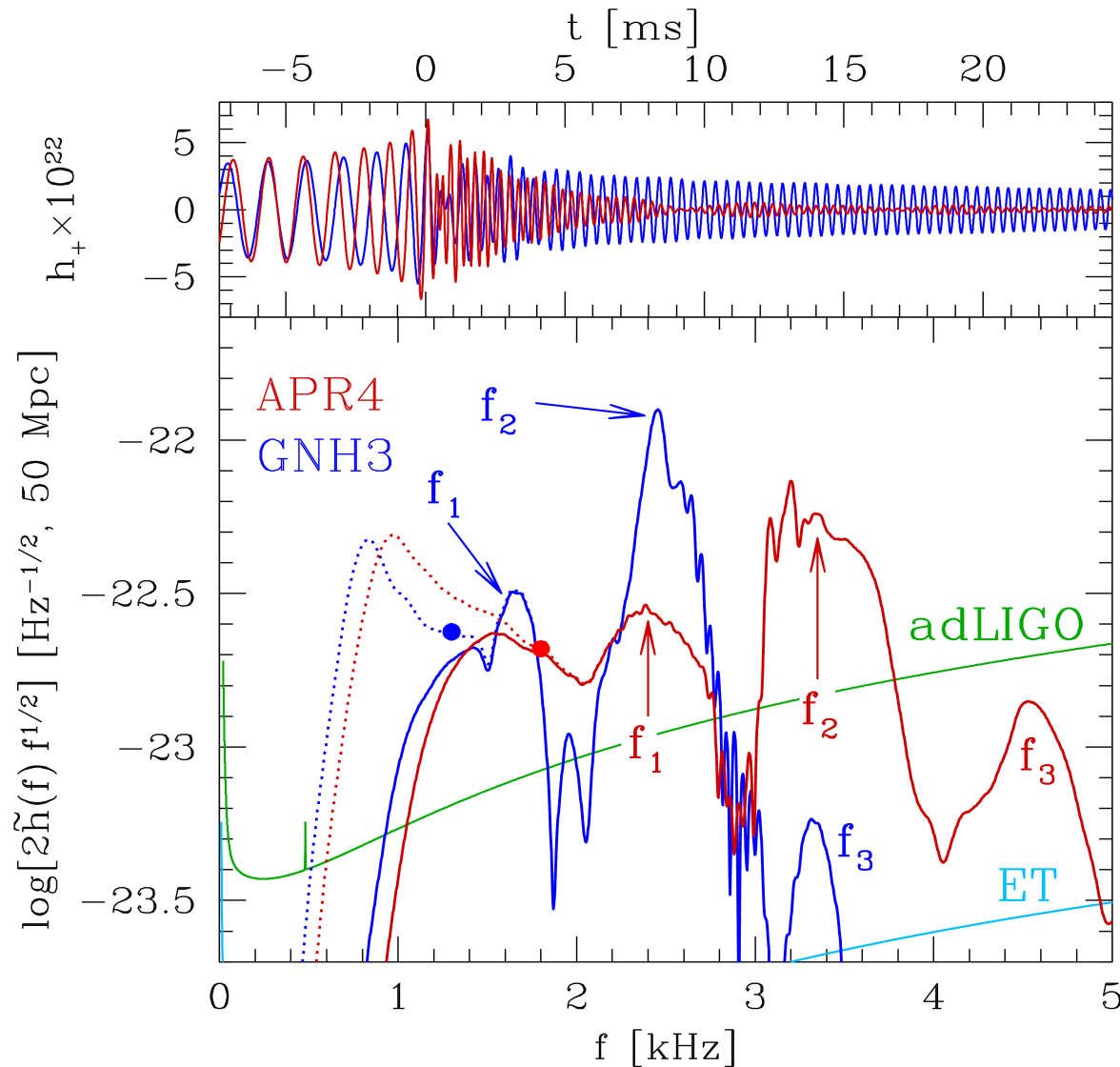
Central value of the lapse function α_c (upper panel) and maximum of the rest mass density ρ_{\max} in units of ρ_0 (lower panel) versus time for the low mass simulations .

EoS: ALF2, $M=1.35$ Post-Merger Phase

Gravitational wave amplitude h_+ and $|h|$ at a distance of 738 km for the ALF2-M135 model



GW-Spectrum for different EoSs



See:

Kentaro Takami, Luciano Rezzolla, and Luca Baiotti, *Physical Review D* 91, 064001 (2015)

Hotokezaka, K., Kiuchi, K., Kyutoku, K., Muranushi, T., Sekiguchi, Y. I., Shibata, M., & Taniguchi, K. (2013). *Physical Review D*, 88(4), 044026.

Bauswein, A., & Janka, H. T. (2012). *Physical review letters*, 108(1), 011101.

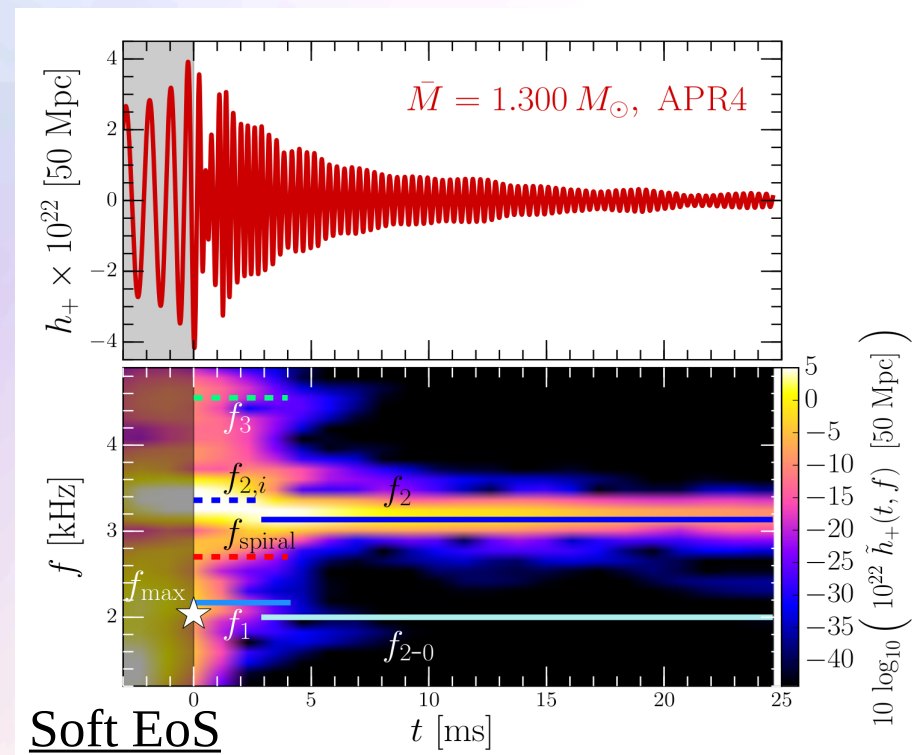
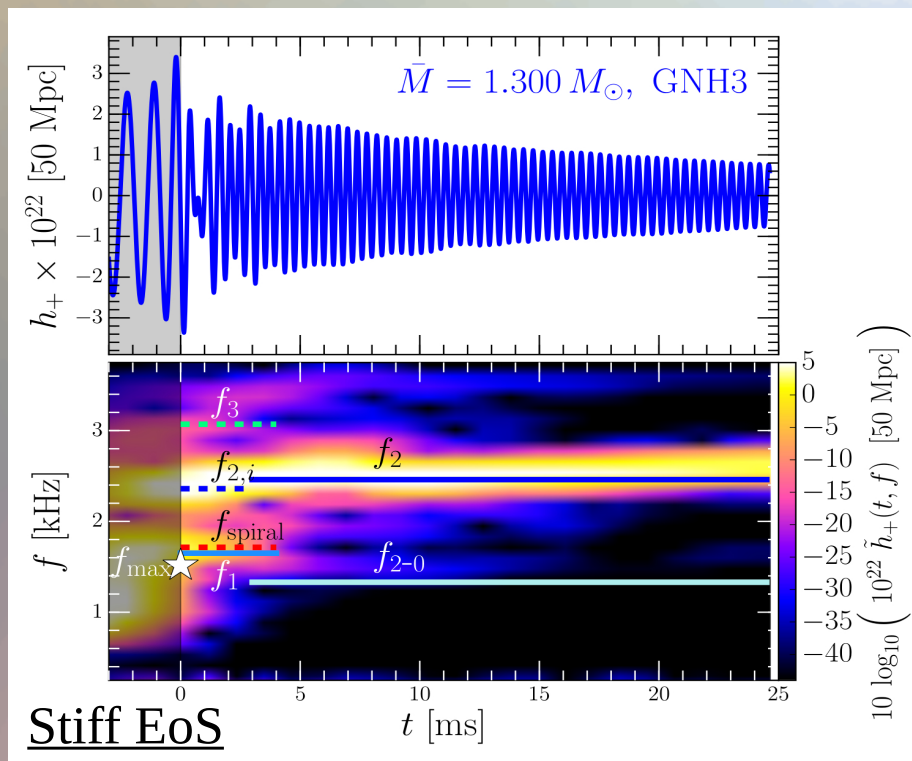
Clark, J. A., Bauswein, A., Stergioulas, N., & Shoemaker, D. (2015). *arXiv:1509.08522*.

Bernuzzi, S., Dietrich, T., & Nagar, A. (2015). *Physical review letters*, 115(9), 091101.

Time Evolution of the GW-Spectrum

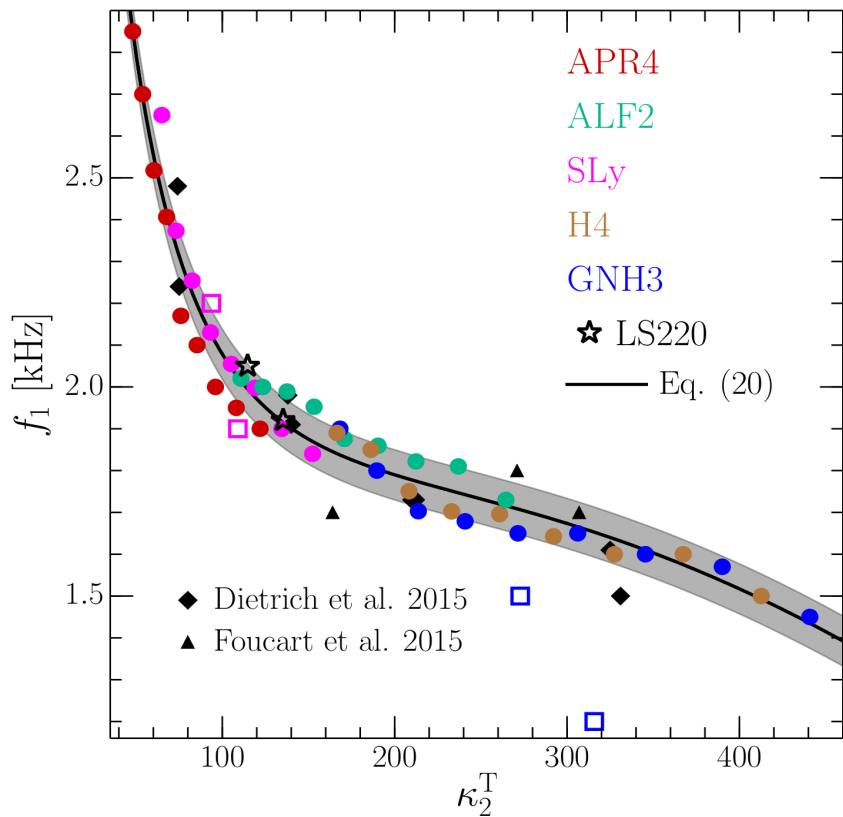
The power spectral density profile of the post-merger emission is characterized by several distinct frequencies f_{\max} , f_1 , f_2 , f_3 and f_{2-0} . After approximately 5 ms after merger, the only remaining dominant frequency is the f_2 -frequency.

See L.Rezzolla and K.Takami, arXiv:1604.00246

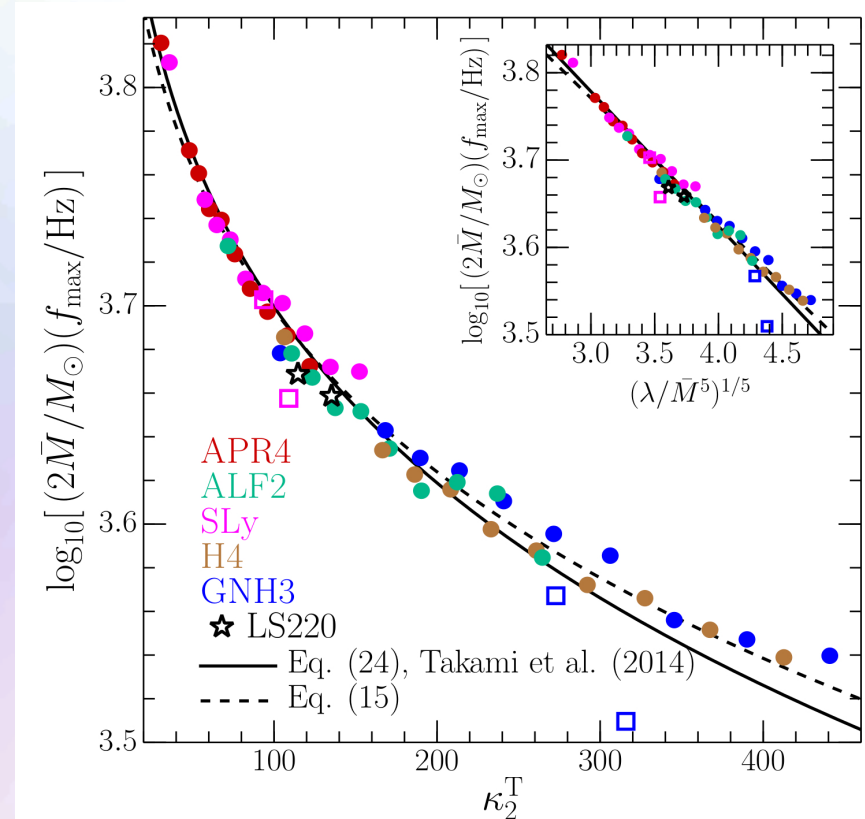


Evolution of the frequency spectrum of the emitted gravitational waves for the stiff GNH3 (left) and soft APR4 (right) EOS.

Universal Behavior of f_1 and f_{\max}

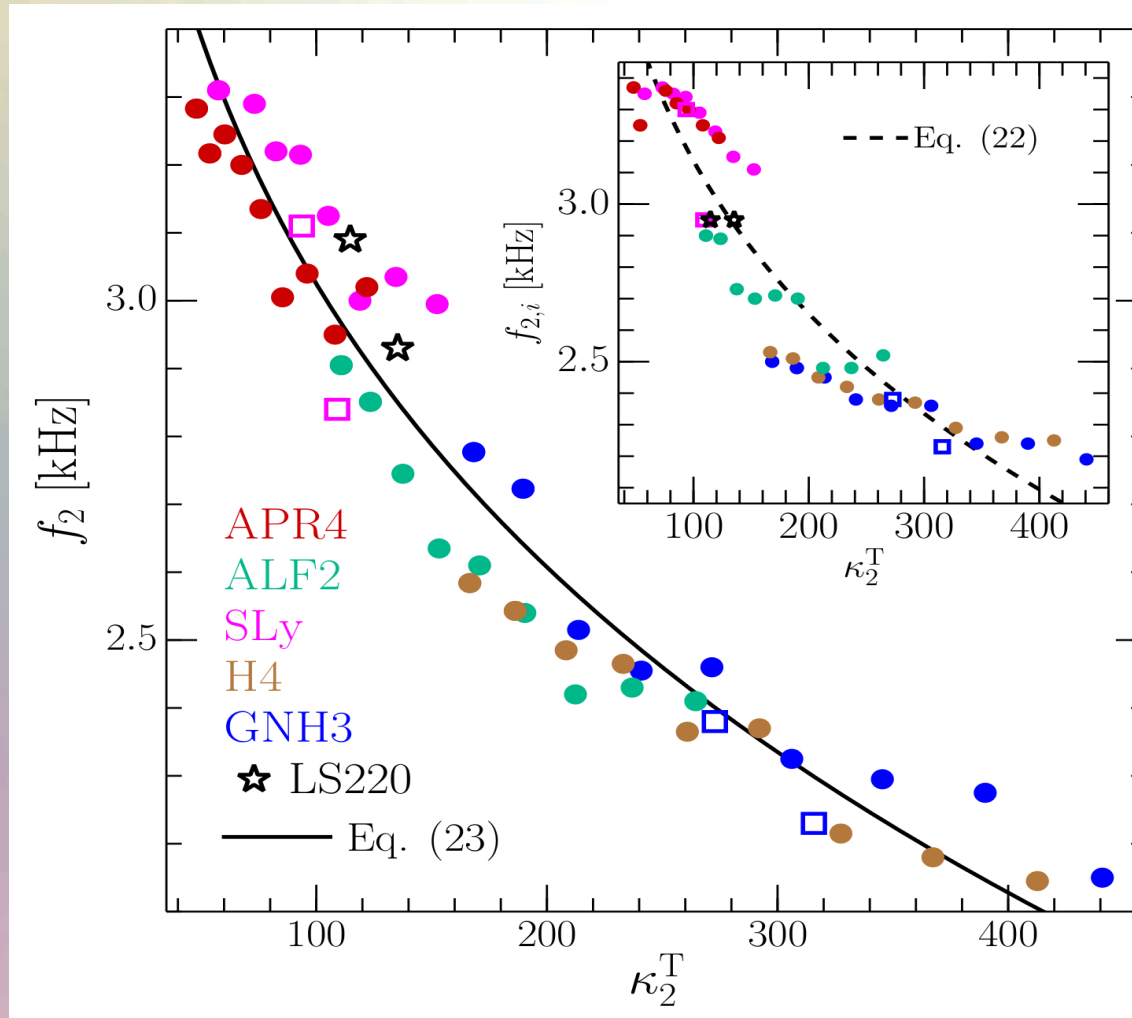


Values of the low-frequency peaks f_1 shown as a function of the tidal deformability parameter κ_2^T .



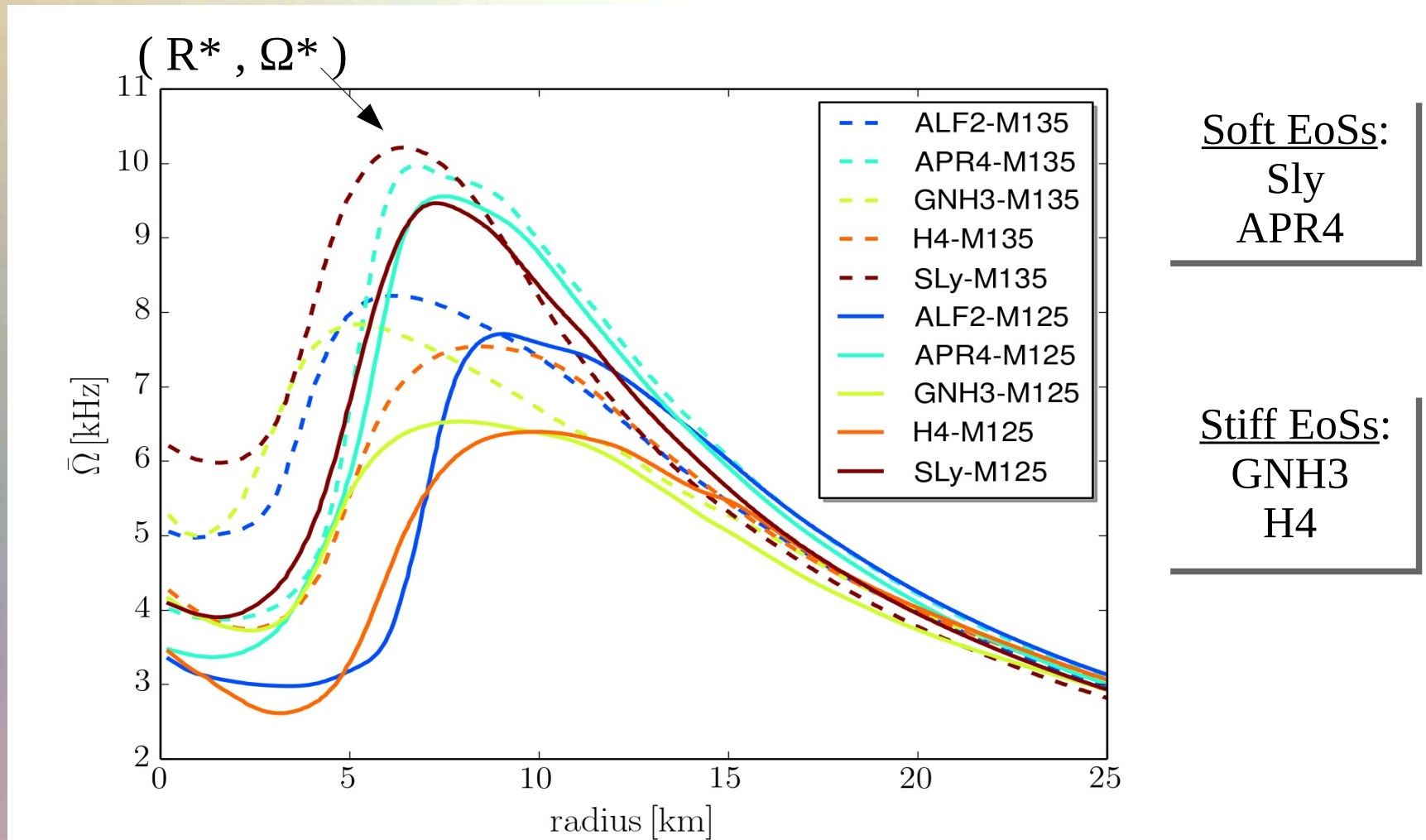
Mass-weighted frequencies at amplitude maximum f_{\max} shown as a function of the tidal deformability parameter κ_2^T .

Universal behavior of the f_2 -peak



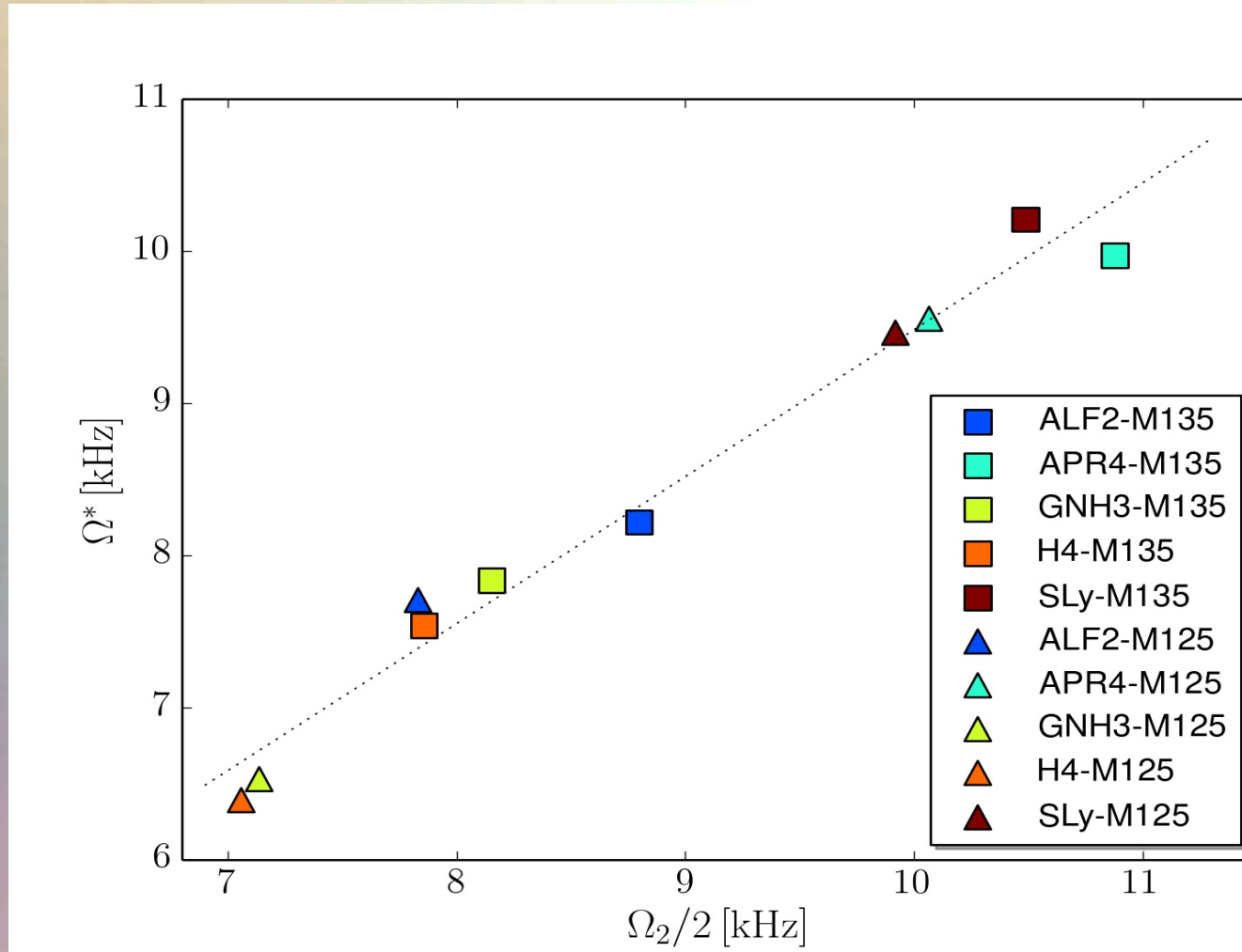
Values of the low-frequency peaks f_2 shown as a function of the tidal deformability parameter κ_2^T .

Time-averaged Rotation Profiles



Time-averaged rotation profiles for different EoS.
Low mass runs (solid curves), high mass runs (dashed curves).

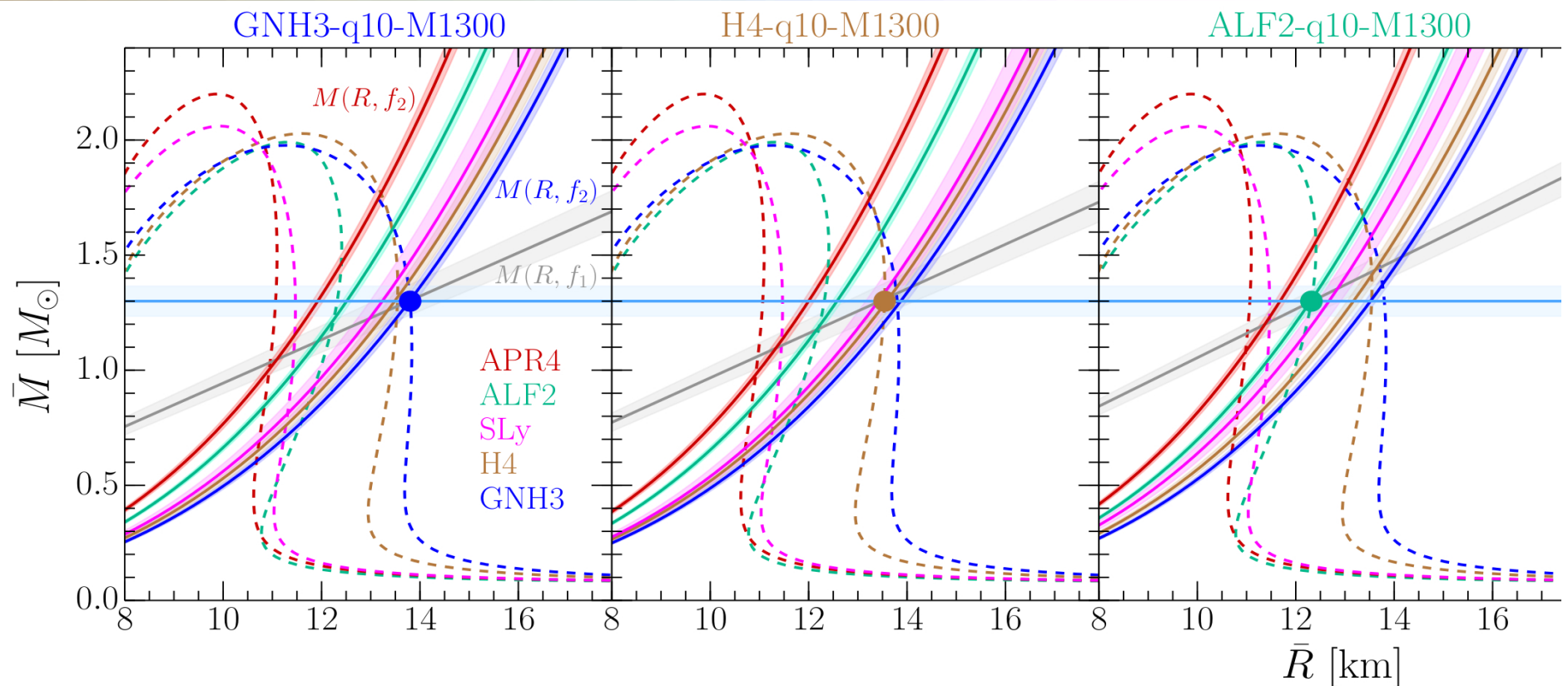
Ω^* versus GW-frequency $\Omega_2 = 2\pi f_1$



Maximum value Ω^* [kHz] of the time-averaged rotation profiles versus the gravitational wave frequency-peak Ω_2 [kHz].

Gravitational Waves → Equation of State

The detection of GWs from merging neutron star binaries can be used to determine the high density regime of the EOS. With the knowledge of f_1 , f_2 and the total mass the system, the GW signal can set tight constraints on the EOS.



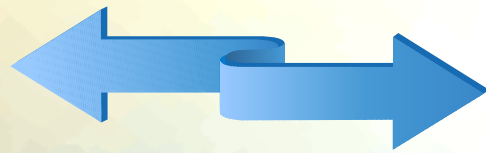
L.Rezzolla and K.Takami, arXiv:1604.00246

K.Takami, L.Rezzolla, and L.Baiotti, Physical Review D 91, 064001 (also PRL 113, 091104)

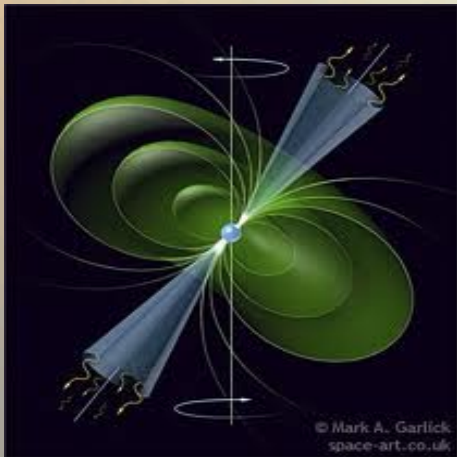
Summary

1. With the first observation of gravitational waves from binary black hole merger by LIGO, the whole branch of observational astronomy will enter a new era - the so called gravitational-wave astronomy.
2. GWs emitted from merging neutron star binaries are on the verge of their first detection.
3. The spectrum of the emitted GWs, within the merger and post-merger phase, depend strongly on the high density regime of the EOS.
4. With the knowledge of the f_1 - and f_2 -frequency peak and the total mass the system, the GW signal can set tight constraints on the EOS.

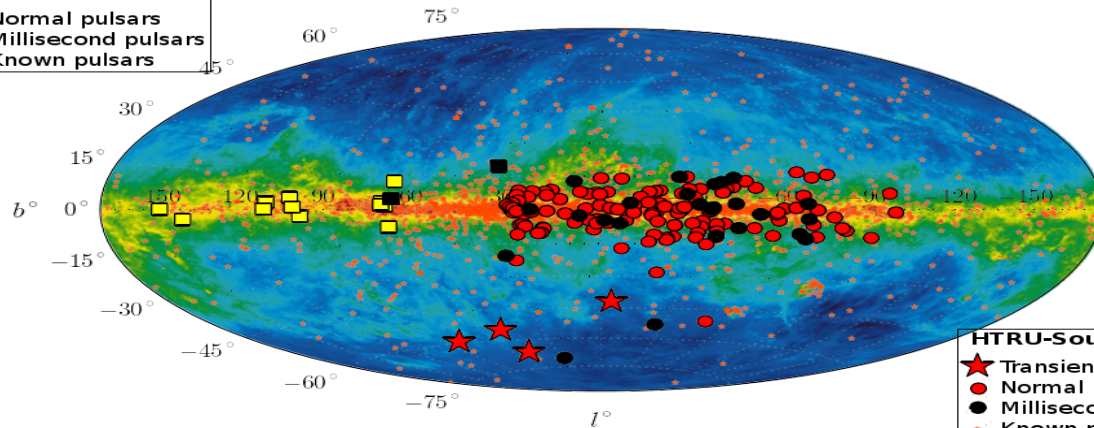
Pulsars



Compact Stars

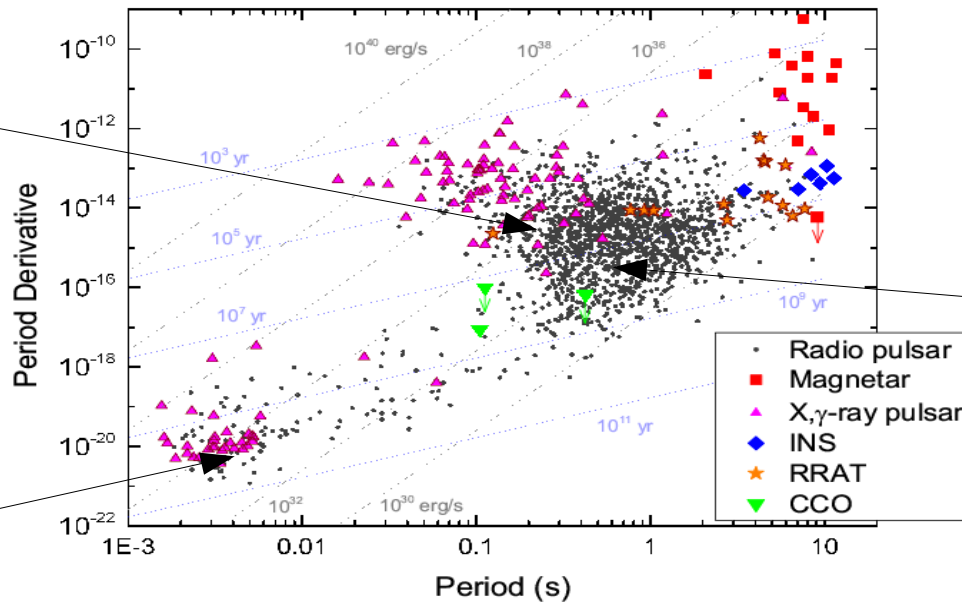


HTRU-North:
 ■ Normal pulsars
 ■ Millisecond pulsars
 * Known pulsars



HTRU-South:
 ★ Transient bursts
 ● Normal pulsars
 ● Millisecond pulsars
 * Known pulsars

PSR B0531+21 (33.5 ms)
Crab Pulsar

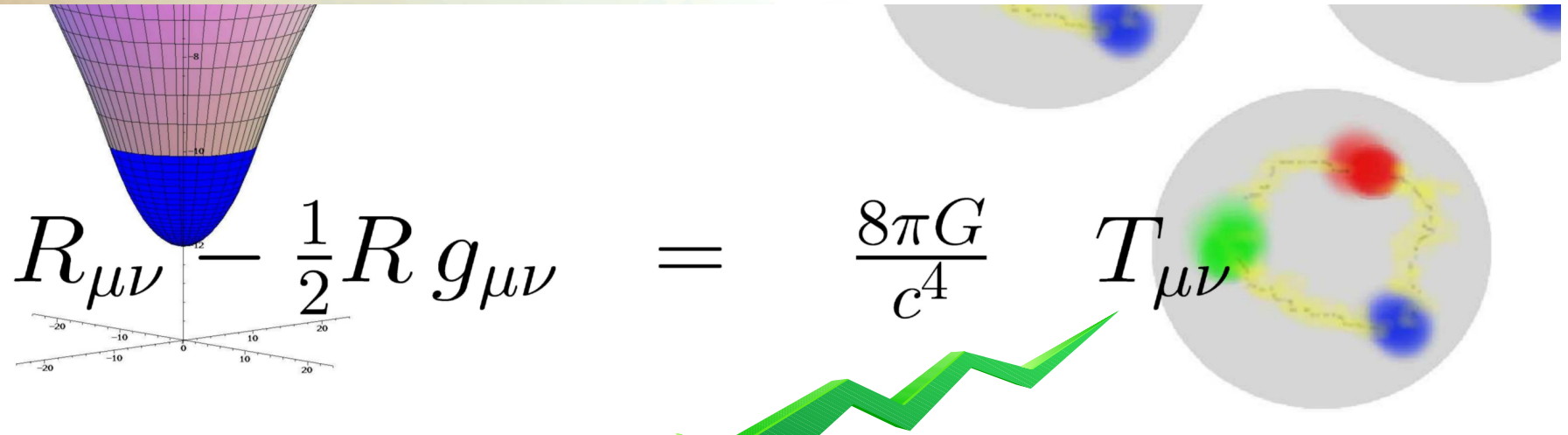


PSR B0329+54 (0.715 s)



PSR B1937+21 (1.56 ms)

Neutron Stars



$$R_{\mu\nu} - \frac{1}{2}R g_{\mu\nu} = \frac{8\pi G}{c^4} T_{\mu\nu}$$

Relativistic Mean-Field Hadronic Models

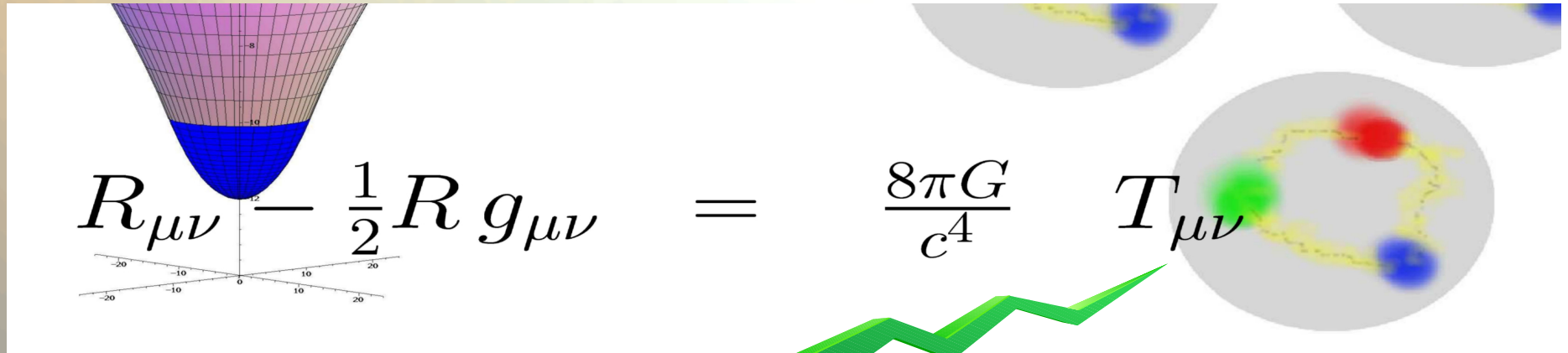
$$\sum_B (p, n, \Lambda, \Sigma^-, \Sigma^0, \Sigma^+, \Xi^-, \Xi^0)$$

$$\begin{aligned} \mathcal{L} = & \sum_B \bar{\psi}_B (i\partial - m_B) \psi_B + \frac{1}{2} \partial^\mu \sigma \partial_\mu \sigma - \frac{1}{2} m_\sigma^2 \sigma^2 - \frac{a}{3} \sigma^3 - \frac{b}{4} \sigma^4 - \frac{1}{4} \omega^{\mu\nu} \omega_{\mu\nu} \\ & + \frac{1}{2} m_\omega^2 \omega^\mu \omega_\mu - \frac{1}{4} \vec{\rho}^{\mu\nu} \vec{\rho}_{\mu\nu} + \frac{1}{2} m_\rho^2 \vec{\rho}^\mu \vec{\rho}_\mu + \sum_B \bar{\psi}_B (g_{\sigma B} \sigma + g_{\omega B} \omega^\mu \gamma_\mu + g_{\rho B} \vec{\rho}^\mu \gamma_\mu \vec{\tau}_B) \psi_B \end{aligned}$$

$$\begin{aligned} \mathcal{L}^{YY} = & \frac{1}{2} (\partial^\mu \sigma^* \partial_\mu \sigma^* - m_{\sigma^*}^2 \sigma^{*2}) - \frac{1}{4} \phi^{\mu\nu} \phi_{\mu\nu} + \frac{1}{2} m_\phi^2 \phi^\mu \phi_\mu \\ & + \sum_Y \bar{\psi}_Y (g_{\sigma^* Y} \sigma^* + g_{\phi Y} \phi^\mu \gamma_\mu) \psi_Y \quad , \end{aligned}$$

$$\mathcal{L}_{\text{lep}} = \sum_{l=e,\mu} \bar{\psi}_l [i\gamma_\mu \partial^\mu - m_l] \psi_l$$

Hybrid Stars



Hadronic Model + Quark Model (eg. NJL model or MIT-Bag model)

Lagrangian density of the NJL model

$$\begin{aligned}
 \mathcal{L} = & \underbrace{\bar{\psi} (i \not{\partial} - \hat{m}_0) \psi}_{\text{Kinetische und Massenbeiträge}} + G_S \underbrace{\sum_{j=0}^8 \left[\left(\bar{\psi} \frac{\lambda_j}{2} \psi \right)^2 + \left(\bar{\psi} \frac{i \gamma_5 \lambda_j}{2} \psi \right)^2 \right]}_{\text{Skalare Wechselwirkung}} \\
 & - G_V \underbrace{\sum_{j=0}^8 \left[\left(\bar{\psi} \gamma_\mu \frac{\lambda_j}{2} \psi \right)^2 + \left(\bar{\psi} \gamma_\mu \frac{\gamma_5 \lambda_j}{2} \psi \right)^2 \right]}_{\text{Vektorielle Wechselwirkung}} \quad \psi \equiv \psi_{Aa}^f \\
 & - K \underbrace{[\det_f (\bar{\psi} (1 - \gamma_5) \psi) + \det_f (\bar{\psi} (1 + \gamma_5) \psi)]}_{\text{Flavour Mischterme}} + \underbrace{\mathcal{L}_L}_{\text{Leptonische Beiträge}}
 \end{aligned}$$

MIT-Bag model

$$\begin{aligned}
 \epsilon^Q &= \sum_{f=u,d,s} \frac{\nu_f}{2\pi^2} \int_0^{k_F^f} k^2 \sqrt{m_f^2 + k^2} dk + B \\
 P^Q &= \sum_{f=u,d,s} \frac{\nu_f}{6\pi^2} \int_0^{k_F^f} \frac{k^4}{\sqrt{m_f^2 + k^2}} dk - B,
 \end{aligned}$$

The Angular Velocity in the (3+1)-Split

The angular velocity Ω in the (3+1)-Split is a combination of the lapse function α , the ϕ -component of the shift vector β^ϕ and the 3-velocity v^ϕ of the fluid (spatial projection of the 4-velocity \mathbf{u}):

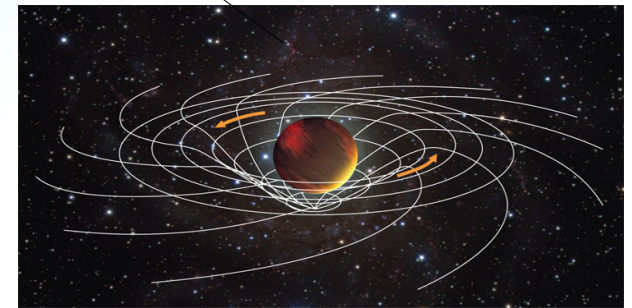
$$\Omega(x, y, z, t) = \frac{u^\phi}{u^t} = \alpha v^\phi - \beta^\phi$$

Angular
velocity Ω

Lapse function
 α

Φ -component
of 3-velocity v^ϕ

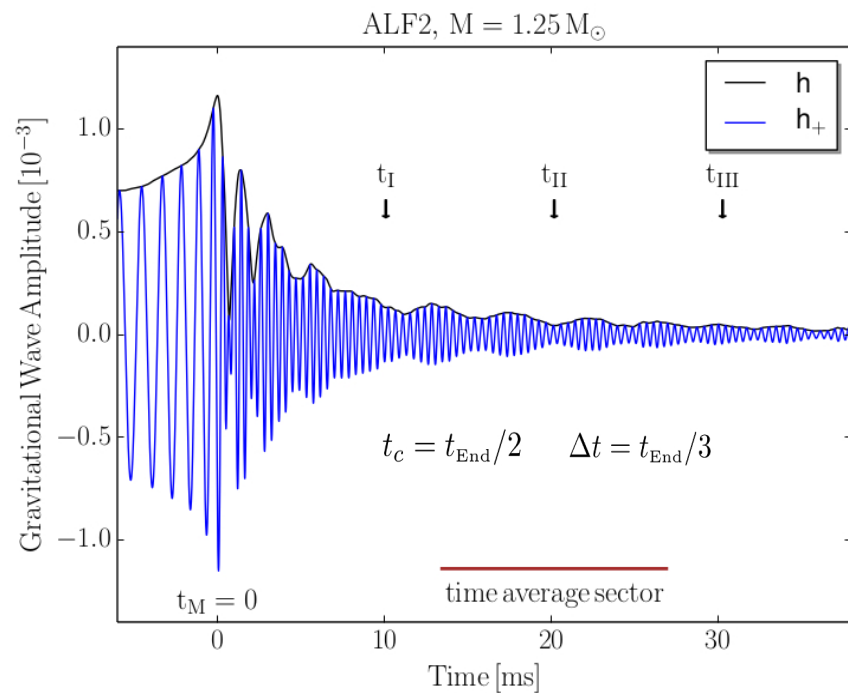
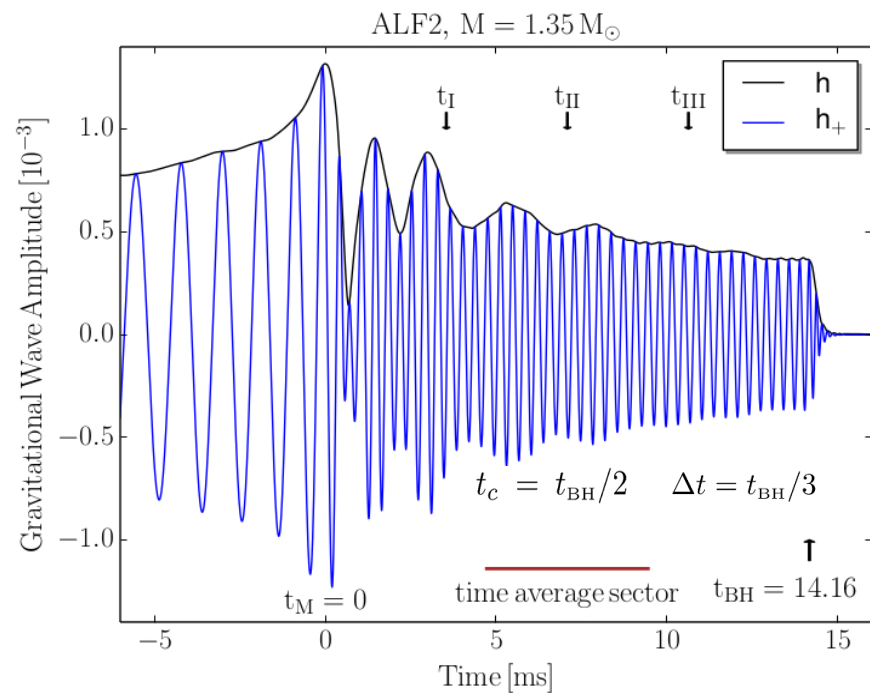
Frame-dragging
 β^ϕ



Focus: Inner core of the differentially rotating HMNS

- M. Shibata, K. Taniguchi, and K. Uryu, Phys. Rev. D 71, 084021 (2005)
- M. Shibata and K. Taniguchi, Phys. Rev. D 73, 064027 (2006)
- F. Galeazzi, S. Yoshida and Y. Eriguchi, A&A 541, p. A156 (2012)
- W. Kastaun and F. Galeazzi, Phys. Rev. D 91, p. 064027 (2015)

Averaging Procedure for Ω



In order to compare the structure of the rotation profiles between the different EOSs, a certain time averaging procedure has been used:

$$\bar{\Omega}(r, t_c) = \int_{t_c - \Delta t/2}^{t_c + \Delta t/2} \int_{-\pi}^{\pi} \Omega(r, \phi, t') d\phi dt'$$

The tidal polarizability parameter κ_2^T

$$\kappa_2^T \equiv 2 \left[q \left(\frac{X_A}{C_A} \right)^5 k_2^A + \frac{1}{q} \left(\frac{X_B}{C_B} \right)^5 k_2^B \right], \quad (11)$$

where A and B refer to the primary and secondary stars in the binary

$$q \equiv \frac{M_B}{M_A} \leq 1, \quad X_{A,B} \equiv \frac{M_{A,B}}{M_A + M_B}, \quad (12)$$

The tidal polarizability parameter κ_2^T

$k_2^{A,B}$ are the $\ell = 2$ dimensionless tidal Love numbers, and $C_{A,B} \equiv M_{A,B}/R_{A,B}$ are the compactnesses. In the case of equal-mass binaries, $k_2^A = k_2^B = \bar{k}_2$, and expression (11) reduces to

$$\kappa_2^T \equiv \frac{1}{8} \bar{k}_2 \left(\frac{\bar{R}}{\bar{M}} \right)^5 = \frac{3}{16} \Lambda = \frac{3}{16} \frac{\lambda}{\bar{M}^5}, \quad (13)$$

where the quantity

$$\lambda \equiv \frac{2}{3} \bar{k}_2 \bar{R}^5. \quad (14)$$

is another commonly employed way of expressing the tidal Love number for equal-mass binaries [32], while $\Lambda \equiv \lambda/\bar{M}^5$ is its dimensionless counterpart and was employed in [34].